*International Journal of Academic Scientific Research*
*ISSN: 2272-6446 Volume 9, Issue 1 (February - March 2021), PP 01-12*
*www.ijasrjournal.org*

# Modeling The Effect of Friction Stir Welding Tool Parameters on Plunge Phase Using Arbitrary Lagrangian-Eulerian Analysis-ALE

**Abdul Mounem Jesri[1], M. Jameel Alshehne[2], Shereen Hesso[1]**

*1 Department of Production Engineering, University of Aleppo, Syria*
*2 Department of Materials Engineering, University of Aleppo, Syria*

***ABSTRACT:*** *A comprehensive understanding of plunge phase is an important step in the optimal design of the friction stir welding (FSW) tool, whereas it plays an effective role in the successful process in terms of sufficient heat generating and material mixing as well as avoiding breakage and wear of the tool, which in turn affects the properties of the resulting weld joint. This paper presents a non-linear, 3D thermo- mechanical coupled model that simulates the plunge phase which is considered the critical phase in the modeling, by using Abaqus/Explicit program, Based on Arbitrary Lagrangian-Eulerian (ALE) analysis with Adaptive Remesh technique, in order to analyze the effect of different tool parameters (shoulder diameter, probe diameter and its height, plunge depth) on the behavior of the plate near the tool and thus the conditions that lead to the successful of the plunge phase in terms of the critical temperature and its distribution of the FSW and stresses applied to the plate. It was found from the numerical results that the welding process with a shoulder diameter of 16 mm ,a probe diameter of 5 mm ,a height of 4.5 mm and with a plunge depth of 0.2 mm were considered the optimal parameters for the tool design that gives the required temperature, which is about (70-90%) of the melting temperature in addition to lower stresses compared to other parameters which were applied to 6061-T6 aluminum alloy at tool rotation speed of 315 Rpm, numerical results were verified by the experimental application throughout using vertical milling machine to produce the welded butt joints and followed by microstructure examination*.

***Keywords -*** *Friction Stir Welding: FSW, 6061-T6, -ALE: Arbitrary Lagrangian-Eulerian Analysis.*

## I. INTRODUCTION

To understand the principle of the FSW, which is considered a high-speed dynamic process, it is necessary to understand the physics related to the heat generation when the tool rotate, where the tool consists of the shoulder and the probe, the shoulder is cylindrical in shape with a specific diameter and the probe is considered the plunge part is characterized by a specific diameter, height and profile geometry [1] as shown in Figure 1[2].

The tool begins to penetrate gradually and continuously at the edge of the two plates until there is contact between the bottom surface of the shoulder and the top surface of the plate (or the specific plunge depth is applied) and therefore heat is generated by frictional heating from the beginning of the contact between the interface surfaces of the tool-plate in addition to the severe plastic deformation around the tool [3]. FSW tool parameters as well as rotation speed of the tool are important parameters which have affecting on the total heat generated and stresses applied to the welded plate.

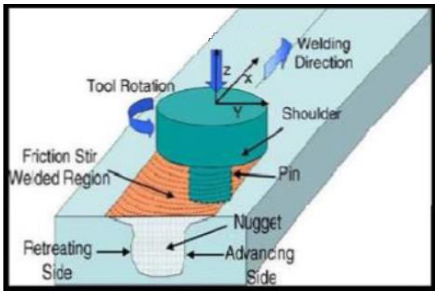


**Figure. 1.** Schematic drawing of FSW [3].

Numerical modeling is often used to obtain the parameters of the optimal tool, but it is a complicated task due to high stress and strain rate at the beginning of the tool-plate contact and this leads to non-linear material behavior, excessive mesh distortion and the need to high computational resources [4]therefore, numerical modeling that simulates the actual process and is based on a suitable analysis approach is a great challenge to overcome the previous problems that often lead to failure and termination of the solution [5].

The analysis approach used in FSW varies to the Lagrangian, Eulerian, coupled Eulerian – Lagrangian(CEL) and finally the Arbitrary Lagrangian-Eulerian (ALE) analysis - with Adaptive Remesh, and each approach has its advantages and disadvantages, but the latter approach is considered the best for the plunge phase, especially when the goal is to study the parameters of the tool, it provides an accurate solution to boundaries and interfaces and maintains a high mesh quality throughout the FSW calculation as long as possible [6].

**ALE analysis**: During the FSW process, severe deformations occur around and below the probe and shoulder which involve a large amount of plastic deformation with a high strain rate. In such a case, the Lagrangian analysis is not suitable for confining large plastic deformation due to excessive mesh distortion, and Eulerian analysis is suitable for solving Computational Fluid Dynamics (CFD) problems and CEL analysis is often used when studying the process at the global level, so one of the most important considerations during FSW simulation is choosing an appropriate analysis approach which determines the ability of the model to overcome large mesh distortions with a satisfactory calculation time.

The ALE analysis combines the advantages of both Lagrangian and Eulerian that means that the node points can be moved arbitrarily, which enables the material to move independently of the mesh [7] making it possible to maintain a high quality mesh during the analysis. Here the topology mesh does not change in the model, which means that the number and connection of elements remains the same [8] and the ALE analysis is the most appropriate approach to investigate the effect of tool parameters when studying the process at the local level. Figure.2 illustrates the approach to analysis of ALE [9].

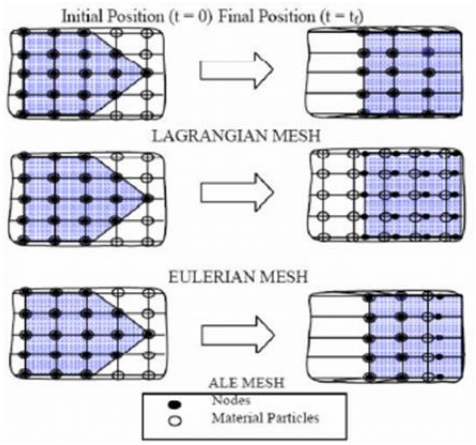


**Figure.2.** The difference in Lagrangian, Eulerian and Arbitrary Lagrangian- Eulerian(ALE) analysis.

There have been some attempts to model the FSW process, taking into account simplifications in building the model. Hongjun et al have developed a model that does not include the mechanical reaction of the tool and thus, was considered a non-mechanical heat source [10] as Elhadj Raouache et al have developed a model to study the only probe profile geometries of the tool based on thermal analysis using COMSOL program [11].

On the other hand, Mandal et al. have used the ALE analysis approach to numerical research of the plunge phase of 2024 alloy with a thickness of 20 mm to measure the axial load on the tool [5]. Lionel Fourment and others in also have used the ALE analysis approach to calibrate the two friction models (Norton's and Coulomb's) of alloy 6061-T6 using the Forge3 program [12].

Attempts to study tool parameters have restricted according to the following research: Keivani et al have implemented a 3D model to study the thermal properties of 1100Cu by studying probe angle and preheating on

temperature distribution using ALE analysis [13] and Raguraman et al have studied the probe profile numerically using ANSYS program for their effect on the steady state of AA 6061 and AZ61 [14]. George et al have studied the plunge phase in the FSW process in order to study the effect of plunge rate and rotation speed on the temperature [15]. After then, Jishnu Padman et al have studied experimentally the effect of the geometry of the probe of the aluminum alloy 6061 of 4 mm thickness on the microstructure and mechanical properties [16].

finally, Aylin Ahadi et al have built a thermo-mechanical model of welding process using the Abaqus program based on ALE analysis and assuming large simplifications in order to reduce the calculation time and the excessive deformation of the elements, where the plunge phase was not taken into account due to the difficulty of modeling it, thus a hole was made in the plate with the dimensions of the probe and in other cases, other methods were adopted to solve the problem of plunge that do not simulate the actual welding process [17].

From previous studies, we have found that modeling of the plunge phase in the FSW process with a complete model that simulates the actual process is an important step in design of the tools and successful of the FSW process, although there were some researches attempting to model the FSW process, they weren't based on creating a real model or did not address the all design parameters of the FSW tool due to the difficulties and challenges facing them in this phase. These issues have been successfully dealt with in this research which avoids all previous problems and builds a more comprehensive model.

## II. OBJECTIVES

The aim of this paper is to study the effect of all FSW tool design parameters by implementing of a non-linear, 3D thermo- mechanical coupled model that integrates the mechanical action of the tool and the thermal- mechanical process of the material in the plunge phase, which represents the highest gradation in FSW with many transformations that it starts with occurrence such as contact, friction, soft material and deformation of material, using explicit/ Abaqus program based on ALE analysis with Adaptive Remesh technique to obtain the optimal design of the FSW tool by the required process temperature, its distribution and also the lowest stresses applied to the studied aluminum plate, and then experimental verification of numerical results and confirmation of the microstructure of the resulting weldment.

## III. METHODOLOGY

1- A numerical model of the FSW process for the plunge phase was performed by Abaqus/ Explicit program with thermo- mechanical coupling based on AEL analysis with the Adaptive Remesh technique.
2- Verification of the effect of the FSW tool parameters by applying the implemented model to different values of shoulder diameter, probe diameter and height, and plunge depth. Finally, the optimal parameters tool that achieve FSW temperature and lower stresses were obtained.
3- Matching the results modeling experimentally by experimental application of the butt joints for 6061-T6 aluminum alloy using a vertical milling machine, and verifying the quality of the resulting joint by microstructure examination.

## IV. NUMERICAL MODLING

**1- Mathematical equations for the FSW process:**

**1-1- The heat transfer equation:** The governing equation that describes the heat transfer equation during the FSW process can be written as follows, Equation (1)[4]:

$$\rho c_p \frac{\partial T}{\partial t} = \frac{\partial}{\partial x}[k_x \frac{\partial T}{\partial x}] + \frac{\partial}{\partial y}[k_y \frac{\partial T}{\partial y}] + \frac{\partial}{\partial z}[k_z \frac{\partial T}{\partial z}] + G \ldots\ldots (1)$$

where ρ is the material density, $c_p$ is specific heat, T is the temperature, t: is the time, k is the heat conductivity, G: is the heat generation.

**1-2- Mechanical Analysis:** Analytically, the mechanical response to FSW is represented by the motion equation as follows Equation (2):

$$M\ddot{w} + C\dot{w} + Kw = F \ldots\ldots (2)$$

Where: M represents mass, C: damping, K: stiffness modulus, F: external force. And also $w^{\cdot\cdot}, w^{\cdot}, w$ is displacement, velocity, and complex acceleration, respectively. The equation above can be written as follows:

$$3) w_i^{\cdot\cdot} = M^{-1}(F - Cw_i - Kw_i) \dots\dots ($$

The explicit central difference equation is used for integration, thus the acceleration equation can be written as follows Equation (4):

$$w_i^{\cdot\cdot} = \frac{w^{\cdot}_{i+\frac{1}{2}} - w^{\cdot}_{i-\frac{1}{2}}}{\Delta t_{i+1} + \Delta t_i/2} \dots\dots (4)$$

As for velocity, it can be expressed in equation as follows Equation (5):

$$w^{\cdot}_{i+\frac{1}{2}} = \left(\frac{\Delta t_{i+1} + \Delta t_i}{2}\right) w_i^{\cdot\cdot} + w^{\cdot}_{i-\frac{1}{2}} \dots\dots (5)$$

Replace the nodal acceleration, we get the velocity equation in the final form, Equation (6)[7]:

$$w^{\cdot}_{i+\frac{1}{2}} = \left(\frac{\Delta t_{i+1} + \Delta t_i}{2}\right) M^{-1}(F - Cw_i - Kw_i) + w^{\cdot}_{i-\frac{1}{2}} \dots\dots (6)$$

**1-3- Material Model**: Johnson-Cook Law is used to describe the plastic behavior as in Equation (7) [18] in addition to a Johnson-Cook damage law to deal with deformation of the Non-natural element, is derived from the law of cumulative damage as in Equation (8) [19]:

$$\sigma y = [A + B(\bar{\varepsilon}^{pl})^n]\left[1 + c\left(\frac{\bar{\dot{\varepsilon}}^{pl}}{\dot{\varepsilon}_0}\right)\right]\left[1 - \left(\frac{T - T_{room}}{T_{melt} - T_{room}}\right)^m\right] \dots\dots (7)$$

where $\bar{\varepsilon}^{pl}$ is the effective plastic strain, $\bar{\dot{\varepsilon}}^{pl}$ is the effective plastic strain rate, $\dot{\varepsilon}_0$ is the normalizing strain rate and A: Yield stress, B:Strain factor, C: Strain rate factor, m: the exponent of temperature, n: the exponent of strain hardening effect, $T_{room}$: is the room temperature, $T_{melt}$ are material solidus temperature, T: Effective temperature.

$$D = \sum\left(\frac{\Delta\varepsilon}{\varepsilon_{failure}}\right) \dots\dots (8)$$

where D is the failure parameter, and the failure is assumed to occur when D is equal to 1.0.14,15 The current failure strain is defined as Equation (9):

$$\varepsilon_{failure} = [D_1 + D_2\exp(D_3\sigma^*)][1 + D_4\ln(\varepsilon^*)](1 + D_5T^*) \dots\dots (9)$$

where $\Delta\varepsilon$ is the increment in the effective plastic strain during an increment in loading, and $\sigma^*$ is the mean stress normalized by the effective stress. The parameters, $D_1$, $D_2$, $D_3$, $D_4$ and $D_5$ are material constants.

**1-4- Mass-scaling method**: To reduce the computing time, a technique called "mass-scaling" was used, Computation time can be reduced by artificially increasing the mass of material (density) without affecting the results, Equation (10):

$$\Delta t = \frac{L_e}{C_d} \dots\dots (10)$$

where Le is the length of the smallest element and $C_d$ is propagation speed of an elastic wave, Equation (11):

$$C_d = \sqrt{\frac{E}{\rho}} \dots\dots (11)$$

where E is the modulus of elasticity and ρ density of the material. The number of increments, n, required is: $n=\frac{T}{\Delta t}$ where T is the natural time of the event. Taking into account the relations (10) and (11), we can say that in Equation (12):

$$n=\frac{T}{L_e}\sqrt{\frac{E}{\rho}} \dots\dots (12)$$

Increasing the density of the material by using a mass scaling factor $f$ is equivalent to reducing the number of increments n to $n/\sqrt{f}$ and thus equivalent to reducing computation time to $T/\sqrt{f}$ [20].

## 2- IMPLEMENTATION OF THE MODEL:

**2-1- Part:** A continuous plate was used in order to avoid contact instability and it was considered a deformable part, and its length and width was decreased to reduce simulation time and maintain its thickness according to the dimensions (80×80×5) mm.

while the tool was considered as a rigid shell discrete part and the probe was selected in a cylindrical shape, fillets were used on the sharp probe edges to reduce stresses concentration and increase the surface of the contact area, parameter study was carried out according to the cases shown in figure. 3 and table 1

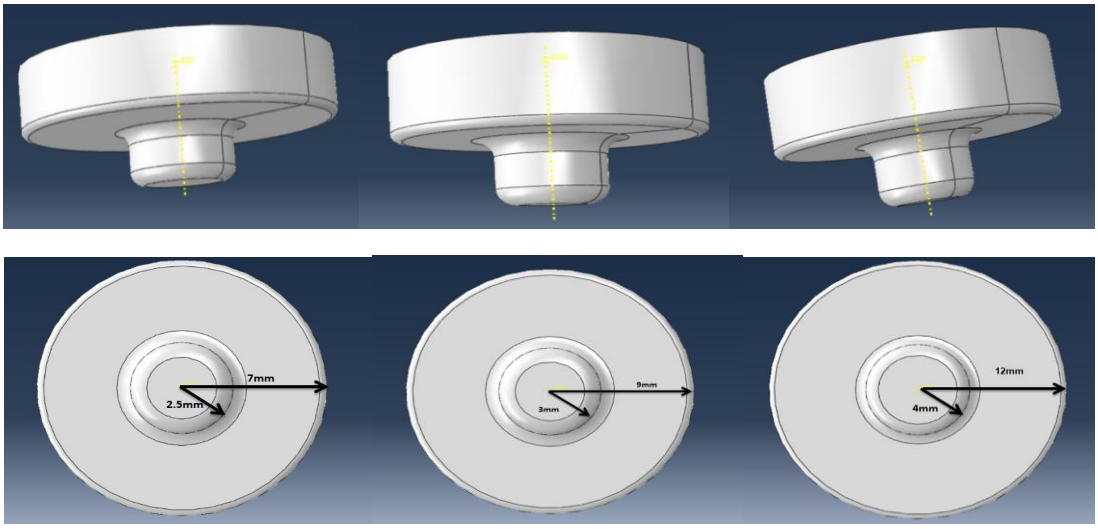


**Figure.3.** The different diameters of the probe and the shoulder of the cylindrical tool.

**Table1.** Parametric Study Cases (probe profile is constant).

| Case | Shoulder diameter | Probe diameter | Probe height | Plunge depth |
|---|---|---|---|---|
| First, the diameters of the shoulder and probe | | | | |
| 1 | 14 | 5 | 4.5 | 0 |
| 2 | 18 | 6 | 4.5 | 0 |
| 3 | 24 | 8 | 4.5 | 0 |
| Second, the Probe height | | | | |
| 4 | 18 | 6 | 3.5 | 0 |
| 5 | 18 | 6 | 4.8 | 0 |
| Third, the plunge depth | | | | |
| 6 | 18 | 6 | 4.5 | 0.3 |

**2-2 Property:** The plate material to be welded was 6061-T6 aluminum alloy. Table 2 shows the parameters of Johnson-Cook law of the plate material while table 3 shows the parameters of Johnson-Cook law of damage. The

physical and thermal properties of the plate were shown according to table 4. Finally, the latent temperature of the alloy was entered as in table 5[21,22].

**Table 2.** Johnson-Coke material parameters for 6061-T6 alloy.

| A | B | C | m | n | Troom | Tmelt |
|---|---|---|---|---|---|---|
| 342 | 114 | 0.002 | 1.34 | 0.42 | 25 | 583 |

**Table 3.** Johnson-Coke damage material parameters for 6061-T6 alloy.

| D1 | D2 | D3 | D4 | D5 | Tmelt | Ttras | Refe Strain Rate |
|---|---|---|---|---|---|---|---|
| 342 | 114 | 0.002 | 1.34 | 0.42 | 583 | 200 | 0.6 |

**Table 4.** Thermal and mechanical properties of 6061-T6 alloys**.**

| Temperature ℃ | Density Kg/m3 | elasticity's Modulus Pa | Poisson modulus | Specific heat J/kgC | Thermal expansion |
|---|---|---|---|---|---|
| 25 | 2690 | 6.69E+10 | 0.33 | 945 | 2.35E-05 |
| 100 | 2670 | 6.32E+10 | 0.334 | 978 | 2.47E-05 |
| 149 | 2670 | 6.13E+10 | 0.335 | 1000 | 2.57E-05 |
| 204 | 2660 | 5.63E+10 | 0.336 | 1030 | 2.66E-05 |
| 260 | 2660 | 5.12E+10 | 0.338 | 1052 | 2.76E-05 |
| 316 | 2630 | 4.72E+10 | 0.36 | 1080 | 2.85E-05 |
| 371 | 2630 | 4.35E+10 | 0.4 | 1100 | 2.96E-05 |
| 427 | 2600 | 2.88E+10 | 0.41 | 1130 | 3.07E-05 |
| 482 | 2600 | 2.02E+10 | 0.42 | 1276 | - |

**Table 5.** Latent Heat parameters for 6061-T6 alloy.

| Latent Heat | Solidus Temp | Liquids Temp |
|---|---|---|
| 3960 | 25 | 583 |

Finally, it was considered that 90% of the plastic deformation is converted to heat.

**2-3-Step**: The analysis was chosen of the type Dynamic Explicit Temperature- Displacement and the mass scaling feature was used to obtain the constant time increment at least step time is 0.0005s. And the Adaptive Remesh variables were also determined in the ALE analysis by performing them for every 10 increments and each remeshing algorithm includes 6 mesh sweeps for optimizing the node positions.

**2-4-Interaction**: The contact between the tool which was considered as the master surface and the plate was considered as the slave surface is surface to surface contact, by frictional slip described by Coulomb's law with a coefficient of friction that varies with temperature as in the table 6, and the normal behavior was described as Hard Contact and in Heat Generation it was considered that the entire frictional action turns into heat but about 30 % of this total heat is transferred to the tool by kinematic contact.

**Table 6.** Temperature dependent friction coefficient of aluminum [23].

| Temperature℃ | Friction Coefficient |
|---|---|
| 22.0 | 0.610 |
| 34.7 | 0.545 |
| 93.3 | 0.259 |
| 147.5 | 0.115 |
| 210.6 | 0.064 |
| 260.0 | 0.047 |
| 315.6 | 0.035 |
| 371.1 | 0.020 |
| 426.7 | 0.007 |
| 583.0 | 0 |

**2-5-Load**: Here, the plate was fixed at the outer sides and bottom surface to simulate fixtures, and was determining the rotation at constant value 315 Rpm that applied on the reference point of the tool according to the plunge phase. And The amplitude in the smooth step pattern was applied for the displacement, the initial temperatures of both the tool and the plate were set at 25℃, the Boltzmann constant 5.766 E-008 and absolute zero temperature -273.15.

**2-6-Mesh**: The mesh was categorized in such a way that there was a higher mesh density around the plunge area, this improves the resolution around the tool without increasing the enormous computational time.

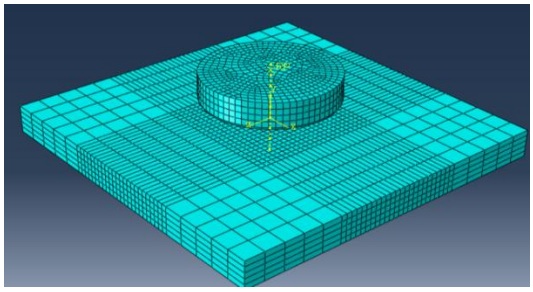

**Figure. 4.** The mesh in the model.

The element type C3D8RT( 8-node thermally coupled brick, trilinear displacement and temperature, reduced integration, hourglass control) was used for the plate and with a gradual element size from 4 to 0.1 mm. while the element type for the tool is R3D4( 4-node bilinear rigid quadrilateral)

The previous modeling steps were performed on eight cases with different tool geometry as shown in Table1. The solution model was 2 days continuous for each case on: Intel (R) Core(TM) i5-8300H CPU@2.30GHZ, 64 bit, 16 Giga bit, Windows 10, Gaming Processor for all phases of welding process.

## VI. RESULT AND DISCUSSION

First, when the effect of the shoulder and the probe diameters were studied, the results of numerical modeling from the AEL model appeared in figures 5,6,7 which were the temperatures and their distribution in addition to the von MSS stresses at the end of the plunge phase for the cases No1.2.3, respectively as in table 1.

Starting from figure 5 which shows the temperature and stress for the case No.1, i.e. the tool with a 14 mm shoulder diameter, 5 mm probe diameter and 4.5 mm probe height.

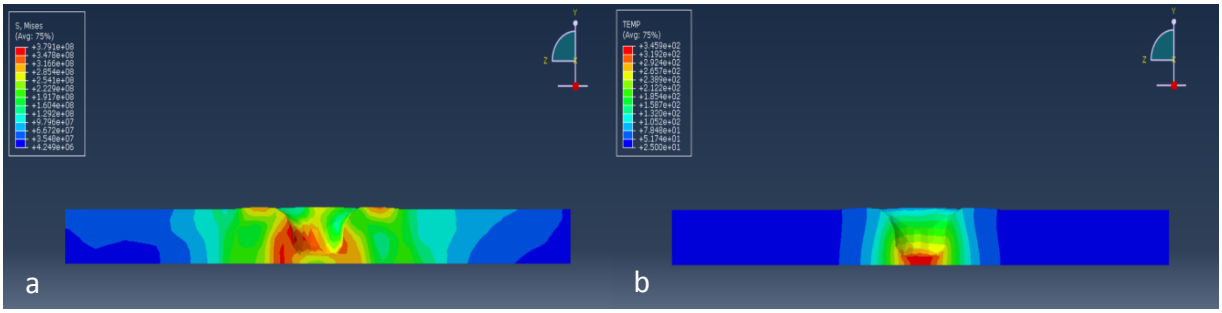


**Figure.5.** a): Temperature, b): von MSS stresses at plunge phase for Case 1.

Figure 6 shows the temperature and stress for case No. 2 with a shoulder diameter of 18 mm and a probe diameter of 6 mm.

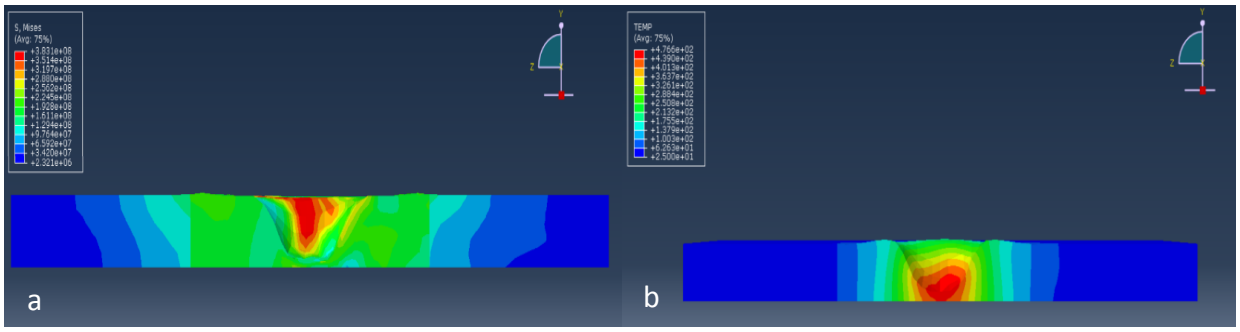


**Figure.6.** a): Temperature, b): von MSS stresses at plunge phase for Case 2.

Figure 7 shows the temperature and stress of the plate for Case No.3 with a shoulder diameter of 24 mm and a probe diameter of 8 mm.

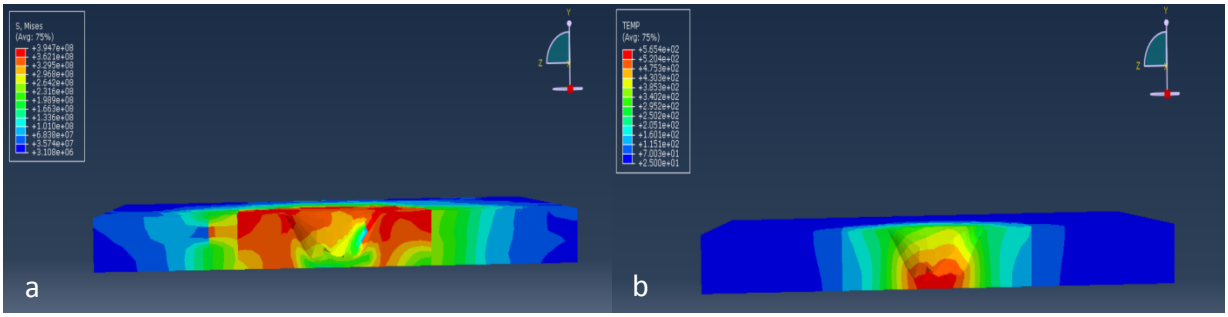


**Figure.7.** a): Temperature, b): von MSS stresses at plunge phase for Case 3.

As for figure 8, it represents the graph of the temperature and von MSS values according to the three studied cases

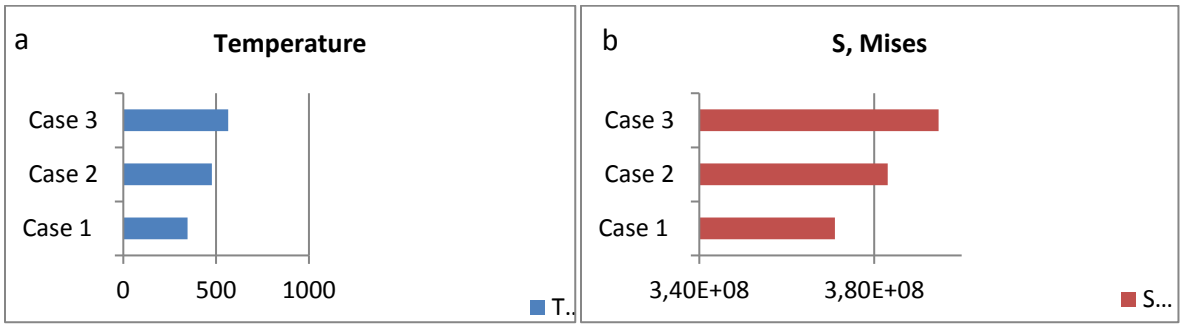


**Figure.8.** Graph representing both a): temperature ,b): Von MSS stresses with changing shoulder and probe diameters.

As for the height of the probe, the studied values were 4,4.5, 4.8 mm, the diameter of the shoulder and the probe have been considered constant 18, 6 mm, respectively. Case No.2 Has been considered to be the case that corresponds to the height of 4.5 mm. As for case No.4, which corresponds to the height of 4 mm, the temperature and stress results shown in figure 9 at the end of the plunge phase.

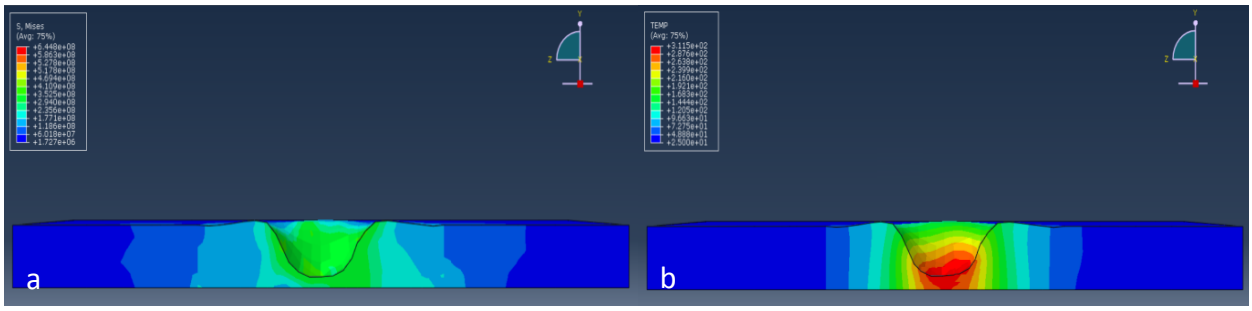


**Figure.9.** a): Temperature, b): von MSS stresses at plunge phase for Case 4.

Figure 10 shows the temperature and stress for case No.5 which corresponding to the probe height of 4.8 mm.

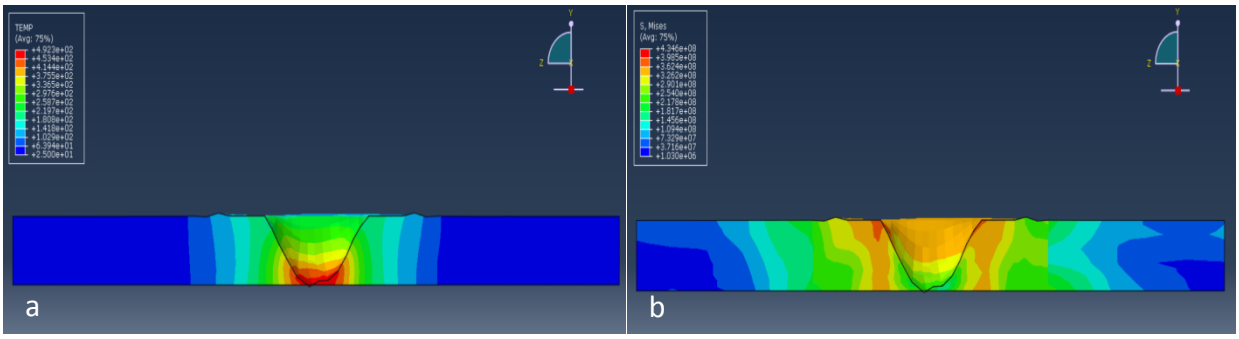


**Figure.10.** a): Temperature, b): von MSS stresses at plunge phase for Case 5.

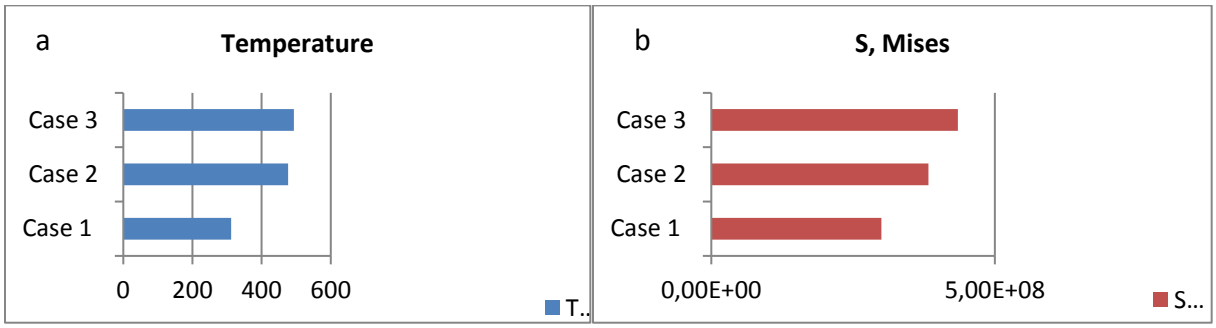


**Figure.11.** Graph representing both a): temperature , b): Von MSS stresses with changing probe height.

Finally, when the plunge depth has been studied, the Shoulder diameter, the probe diameter and height have been considered constant (18, 6, 4.5) mm, however plunge depth has been applied of 0.2 mm into the plate. Figure 12 shows the temperature and stress at the end of the plunge phase for this case.

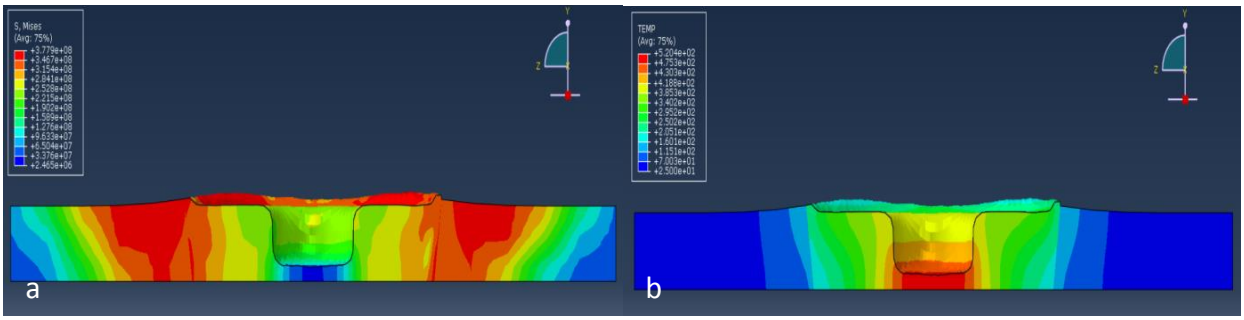


**Figure.12.** a): Temperature, b): von MSS stresses at plunge phase for Case 6.

Now we discuss the results that were presented previously, we observe from the figures 5,6,7 that with increasing both the shoulder and probe diameters, the area of the interface increases and thus the amount of heat produced by the frictional contact, the plastic deformation as well as increases Von Mess stress, leads to the expansion of the weld seam. According to the results that collected in figure 8, we found that the maximum temperature of the plate for the tool with a shoulder diameter of 18 mm and the probe 6 mm was 476.7C°,what achieved the FSW process temperature about.(70-90)% melting point , i.e. was not exceed this range of the studied alloy, while The tool with a shoulder diameter of 22 mm and a probe of 8 mm generated a high temperature close to the melting point in order to increase the area of the interface: probe - plate, shoulder - plate , as for the tool with a shoulder diameter of 14 mm and a probe diameter of 5 mm, the maximum temperature was much lower, because of the frictional interface was small and thus the heat generated is lower which maybe leads to the failure of the FSW process. Also the von MSS stresses to which the plate is subjected, have the same behavior as shown in this figures, where it increases in the value and distribution with the increase both shoulder and probe dimeters, the slight asymmetry also noticed of the temperature and stresses on either side of the advanced and retreating sides. finally, the tool in case No. 2 gave an average value between the other two cases.

On the other hand, for the effect of the probe height have studied was summarized by the figure11, generally the probe height had a slight effect on the maximum temperature during FSW process compared to the shoulder and probe diameters, but both temperature and stress values have shown a more clarification difference between the studied values, where increased when the height was large and when the experimental application maybe leads to defects in the weld joint root, in contrast, small probe height leads to less stirring and low heat generation, resulting to the potential for breaking the tool. Accordingly, the tool with a probe height of 4.5 mm have considered the best among the studied cases.

In general, that plunge depth works to provide the forging force required for the welding process at the experimental application, and it often applied when position control is instead of force control. So we have studied it in the numerical modeling in this paper, i.e. applying a plunge depth of 0.3 mm, the maximum temperature of the plate has risen but it was within the temperature range of the FSW process for the selected aluminum alloys.

According to the results of the numerical modeling, the tool has selected with a shoulder diameter of 18 mm, a probe diameter of 6 mm, and a height of 4.5 mm and the application of a plunge depth of 0.3 mm.

In order to validate numerical results, various welding operations were performed on a modified vertical milling machine that simulates a FSW machine, using a welding tool designed and manufactured according to what was mentioned above as figure 13. H13 tool steel material was used to manufacture the tool, then heat treatment was performed to raise its hardness from (22) HRC to (55) HRC that was suitable for FSW tool.

**Figure .13.** FSW tool.

Then the equipment and the tool were assembled, suitable fixture was applied to prevent plate vibration, and finally the welding process was carried out. A sample was taken from the welding joint and the stirring area was examined using a light microscope as in figure 14, after appropriate preparation of the tested sample.

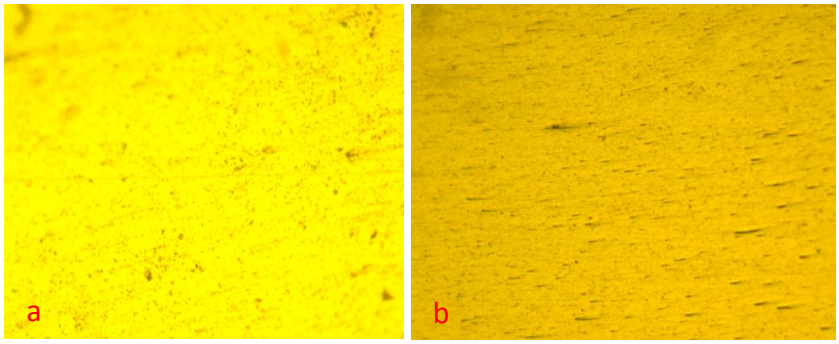


**Figure.14.** a): Base metal, b): Nugget Zone

The image of the microstructure showed that the FSW process has produced a structure with fine equiaxial grains because of the recrystallization process that occurs as a result of the severe plastic deformation and temperature of FSW process. Also the $Mg_2Si$ particles were more uniformly distributed, this mean that temperature was suitable and thus the success of the welding process according to the numerical modeling.

## VI. CONCLUSIONS

1- Numerical modeling was successfully implemented and overcoming the problem of severe mesh distortion resulting from high strain rates in the FSW process, especially the plunge phase, with an acceptable calculation time using ALE analysis with Adaptive Remesh technique at the local level study compared to the CEL analysis method that it is used for the global level study (rotating and traverse speeds) [24].

2- It was found from the results of numerical modeling that heat generation increases by increasing the diameter of the shoulder and the probe, in order to increase the area of contact of the frictional interface, and this result is consistent with the research in the reference [25, 26].

3- From the parametric study in this paper, the tool with an optimal design is with a shoulder diameter of 18 mm, a probe diameter of 6 mm and a probe height of 4.5 mm, and applying a plunge depth of 0.3 mm.

4- Examination of the microstructure after experimental application with the tool manufactured according to numerical results, fine equiaxed grain due to dynamic recrystallization in the nugget zone were obtained and this corresponds to the results of the research in the reference [26, 27].

## REFERENCES

[1] J.T. Khairuddin, J. Abdullah, Z. Hussain, I. P. Almanar, Principles and Thermo-Mechanical Model of Friction Stir Welding, *Welding Processes*-2012, 191-216.
[2] Y. Sharma, Dr. k. Jit Singh, H. Vasudev, Review Paper on Friction Stir Welding and Metal Inert Gas Welding of Aluminium Alloys, *International Journal of Advanced Science and Technology Vol. 29, No. 8s*- 2020, pp. 3341-3348.
[3] F. Panzer, M. Werz, S. Weihe, Experimental Investigation of The Friction Stir Welding Dynamics of 6000 Series Aluminum Alloys, *Production Engineering,12(5)*-2018, 667-677.
[4] R. Česnavičius, S. Kilikevičius, P. Krasauskas, R. Dundulis, H.Olišauskas, Research of The Friction Stir Welding Process of Aluminium Alloys, *MECHANIKA, 22(4)*-2016, 291-296.
[5] S. Mandal, J. Rice, A. Elmustafa, Experimental and Numerical Investigation of The Plunge Stage in Friction Stir Welding, *Journal of materials processing technology, 203(1-3)*- 2008, 411-419.
[6] M. A. Ansari, A Samanta, R. A. Behnagh, H. Ding, An Efficient Coupled Eulerian-Lagrangian Finite Element Model for Friction Stir Processing, *The International Journal of Advanced Manufacturing Technology*, 101(5-8)-2019,1495-1508.
[7] S. B. Aziz, M. W. Dewan, D. J. Huggett, M. A. Wahab., A. M. Okeil, T. W. Liao, A Fully Coupled Thermomechanical Model of Friction Stir Welding (FSW) And Numerical Studies on Process Parameters of Lightweight Aluminum Alloy Joints. *Acta Metallurgica Sinica (English letters), 31(1)*- 2018. 1-18.
[8] R. Hamilton, D. MacKenzie, H. Li, Multi-Physics Simulation of Friction Stir Welding Process, Engineering Computations-2010.
[9] B. Meyghani, M. B. Awang, S. S. Emamian, M. K. B. Mohd Nor, S. R. Pedapati, A Comparison of Different Finite Element Methods in the Thermal Analysis of Friction Stir Welding (FSW), Metals,7(10)- 2017, 450.
[10] H. Li, D. Liu, Simplified Thermo-Mechanical Modeling of Friction Stir Welding with a Sequential Method, *International Journal of Modeling and Optimization*, *4*(5)- 2014, 410.

[11] [E. Raouache, Z. Driss, M. Guidara, F. Khalfallah, Effect of The Tool Geometries on Thermal Analysis of the Friction Stir Welding, International Journal of Mechanics and Applications, 6(1)- 2016, 1-7.
[12] M. Assidi, L.Fourment, S.Guerdoux, T.Nelson, Friction Model for Friction Stir Welding Process Simulation: Calibrations From Welding Experiments, International Journal of Machine Tools and Manufacture, 50(2) -2010, 143-155.
[13] R. Keivani, B. Bagheri, F. Sharifi, M. Ketabchi, M.Abbasi, Effects of Pin Angle and Preheating on Temperature Distribution During Friction Stir welding Operation, Transactions of Nonferrous Metals Society of China, 23(9)-2013, 2708-2713.
[14] D.Raguraman, D.Muruganandam, L. A. Kumaraswamidhas, Study of Tool Geometry on Friction Stir Welding of AA 6061 and AZ61, In Proceedings of National Conference on Contemporary Approaches in Mechanical, Automobile and Building sciences IOSR J Mech Civ Eng-2014., pp. 63-69.
[15] G. Papazafeiropoulos, A. M. Tsainis, Numerical Modeling of The Friction Stir Welding Process, In The 8th GRACM International Congress on Computational Mechanics, Volos, Greece-2015, July, pp. 12-15.
[16] G. Nawaz Ahmad, J. Padman, M.Shahid Raza, A. Kumar, N. K.Singh, Analyzing the Effect of Tool Pin Design and Process Parameters on The Microstructural and Mechanical Properties of Friction Stir Welded 6061 Aluminum alloy, International Conference on Mechanical, Materials and Renewable Energy 377(1)- 2018.
[17] A. Ahadi, F.Roura Port, Fully Coupled Thermo-Mechanical Modelling of the Initial Phase of the Friction Stir Welding Process Using Finite Element Analysis, Advances in Materials Science and Engineering, 2(1) - 2019, 22-22.
[18] V.Malik, N. K.Sanjeev, H. S. Hebbar, S. V. Kailas, Investigations on The Effect of Various Tool Pin Profiles in Friction Stir Welding Using Finite Element Simulations, Procedia Engineering 97 -2014, 1060-1068.
[19] M.Yu, W.Li, J. Li, Y.Chao, Modelling of Entire Friction Stir Welding Process by Explicit Finite Element Method, Materials Science and Technology, 28(7)- 2012, 812-817.
[20] M. Iordache, C. Bădulescu, E. Nițu, D. Iacomi, Numerical Simulation of Friction Stir Welding (FSW) Process Based on ABAQUS Environment. In Solid State Phenomena, Switzerland, Vol. (254)- 2016, pp. 272-277.
[21] M. safari, J. Joudaki, Coupled Eulerian-Lagrangian (CEL) Modeling of Material Flow in Dissimilar Friction Stir Welding of Aluminum Alloys, Iranian Journal of Materials Forming, 6(2)-2019, 10-19.
[22] Z. Zhu, M. Wang, H. Zhang, X. Zhang, T. Yu and Z. Wu, A Finite Element Model to Simulate Defect Formation During Friction Stir Welding, Metals,7(7)- 2017, 256.
[23] M. AWANG, V. H. Mucino. Thermo-mechanical modeling of friction stir spot welding (FSSW) process: use of an explicit adaptive meshing scheme. SAE Technical Paper- 2005.
[24] A. M. Jesri, M. J Alshehne, Sh Hesso, Modeling The Effect of Rotation and Traverse Speeds on Full Friction Stir Welding Process Using Coupled Eulerian- Lagrangian Analysis, International Journal of Academic Scientific Research ISSN: 2272-6446 Volume 8, Issue 4 (November – December)- 2020, PP 39-48.
[25] K. Ramanjaneyulu, G. M. Reddy, A. V Rao, Role of Tool Shoulder Diameter in Friction Stir Welding: An Analysis of the Temperature and Plastic Deformation of AA 2014 Aluminum Alloy. Transactions of the Indian Institute of Metals, 67(5)- 2014,769-780.
[26] N. Z. Khan, A. N Siddiquee, Effect of shoulder diameter to pin diameter (D/d) ratio on tensile strength of friction stir welded 6063 aluminium alloy, Materials Today: Proceedings, 2(4-5)-2015, 1450-1457.
[27] R. M. Vaidyanathan, M. Patel, N. Sivaraman, M. Markos, T. Alemayehu, Micro Structural Evaluation of Friction Stir Welded Aluminium Alloy 6063, International Journal of Recent Technology and Engineering (IJRTE) ISSN: 2277-3878, Volume-8 Issue-2, July-2019.